JOURNAL OF MATERIALS SCIENCE **38** (2003) 4523–4534

Effect of solution heat treatment and additives on the hardness, tensile properties and fracture behaviour of Al-Si (A413.1) automotive alloys

M. A. MOUSTAFA
Central Metallurgical Research and Development Institute, Helwan, Cairo, Egypt; Département des sciences appliquées, Université du Québec à Chicoutimi, Chicoutimi, Québec, Canada G7H 2B1

F. H. SAMUEL
Département des sciences appliquées, Université du Québec à Chicoutimi, Chicoutimi, Québec, Canada G7H 2B1
E-mail: fhsamuel@uqac.ca

H. W. DOTY
GM Powertrain Group, Metal Casting Technology Inc., Milford, NH 03055, USA

A study was carried out to determine the role of Mg, Cu, Be, Ag, Ni, and Zn additives during the solution heat treatment of grain refined, Sr-modified eutectic A413.1 (Al-11.7% Si) alloy, and their consequent effect on mechanical properties. For comparison purposes, some of the alloys were also studied in the non-modified condition. The alloys were cast in the form of test bars using a steel permanent mold preheated at 425°C that provided a microstructure with an average dendrite arm spacing (DAS) of ~22 μm. The test bars were solution heat treated at 500 ± 2°C for times up to 24 h, followed by artificial aging at 155°C for 5 h (T6 treatment). Tensile and hardness tests were carried out on the heat-treated test bars. Details of the microstructural evaluation are reported in a previous article [1].

With respect to the mechanical properties, it is found that the hardness and strength (YS, UTS) of Mg-containing alloys decrease with the addition of Sr due to the sluggish dissolution of the $Al_5Cu_2Mg_8Si_6$ phase during solution treatment, and a delay in the precipitation of Mg_2Si or Al_2MgCu phases during artificial aging thereafter. The properties of the Cu-containing alloys, however, remain unaffected by the addition of Sr. With the exception of Ni, all alloying elements used improve hardness and strength, particularly after heat treatment. In the case of Ni, addition of up to 1.41% Ni is observed to decrease the mechanical properties in the T6 condition.

Fracture of non-modified alloys takes place through crack initiation within the brittle acicular Si particles without the crack passing through the ductile Al matrix. In the Sr-modified alloys, the fracture is of ductile type, as evidenced by the pinpoint nature of the α-Al dendrites on the fracture surface. The number of cracked Si particles and intermetallics beneath the fracture surface increases in proportion to the increase in alloy strength.

1. Introduction

The primary advantages of using aluminum alloys for automotive components include their lightweight, reduced fuel energy consumption and low recycling costs. Environmental concerns have put the onus on automotive manufacturers to develop still lighter and more fuel-efficient vehicles. In this regard, the development of new alloys (and new techniques) has been an ongoing process, where investigations carried out worldwide by aluminum suppliers, R&D organizations, and by the automotive industry have led to the use of these newly developed materials in the production of autobody panels, spaceframes, cylinder heads of turbo-charged diesel engines, brake rotors, suspension parts and other applications [2–6]. Miller *et al.* [7] have provided a pertinent review of the recent developments in aluminum alloys for the automotive industry.

Aluminum-silicon (Al-Si) alloys, in particular, are well known for their excellent castability and strength. The addition of Mg, Cu and Zn makes them heat-treatable, providing the means to enhance the properties using appropriate heat treatments [8, 9]. As the mechanical properties are largely determined by the cast microstructure (characteristics and constituents), the

changes produced in the latter after heat treatment [10, 11] will likewise also affect the properties. In the case of aluminum sheet materials (i.e., wrought alloys), in addition to the microstructure, the alloy properties are also controlled by the crystallographic texture [12, 13]. In such applications, the most important material characteristic is the alloy formability. Hayashi and Nakagawa [14] have reviewed recent trends in sheet metals used in the manufacture of automotive panels.

In the first part of this work [1], the authors reported on the changes in the microstructure (i.e., with respect to intermetallics and silicon particle characteristics) with the addition of Mg, Cu, Be, Ag, Ni and Zn to A413.1 alloy following solution heat treatment at different times at 500°C. Phase identification of the intermetallics observed was carried out using electron probe microanalysis (EPMA). The results showed that 0.42 wt% Mg addition produced large Si particles compared to the base A413.1 alloy; their size was not affected by an increase in solution treatment time or Mg content. Among intermetallics, both Mg_2Si and Al_2Cu dissolved after 8 h, while the β-Al_5FeSi phase underwent partial dissolution and $Al_5Cu_2Mg_8Si_6$ and α-$Al_{15}(Mn,Fe)_3Si_2$ (or α-Fe) phases persisted after 24 h solution time. The presence of Ni and Cu (dissolved) in the α-Fe phase stabilized the phase during solution treatment. The effect of Sr on the β-Al_5FeSi platelets intensified in the presence of Zn.

This article discusses the mechanical properties resulting from the addition of Mg, Cu, Be, Ag, Ni and Zn to A413.1 alloy following solution heat treatment at different times at 500°C. The mechanical properties (hardness and tensile properties) observed have been explained in terms of the dissolution and changes in morphology and volume fractions of the alloy microconstituents that take place, following specific solution treatment times at 500°C.

2. Experimental procedure

All experiments were conducted on A413.1 alloy (coded M0), received in the form of 12.5 kg ingots. The chemical composition is shown in Table I. The experimental procedure involved the preparation of 40 kg melts using a SiC crucible heated in an electric resistance furnace. The melting temperature was kept at 725 ± 5°C. Measured amounts of Cu, Mg, Ag, Ni, Zn and Be alloying elements were added to the base alloy (M0 melt) in the form of master alloys. Only Mg was added in the form of pure metal. All alloys were grain refined with TiB_2 and modified with Sr. In certain cases, for comparison purposes, the alloys were grain-refined but not modified, viz., M2N, M3N, M4N and 1NN alloys in Table I. All melts were degassed using argon injected into the melt by means of a rotating graphite degassing impeller (30 min at 125 rpm).

The alloys listed in Table I are grouped into three categories to facilitate discussion of the results: (i) the base A413.1 alloy, M0, (ii) alloys M1 through M3N, with M1 (viz., Sr-modified M0 alloy) representing the base or reference alloy for this group, and (iii) alloys M4 through ZN, having M4 as their reference alloy.

Tensile test bars (gauge length 50 mm; cross-section diameter 12.7 mm) were produced by pouring the degassed molten metal into a preheated steel permanent mold (type ASTM B-108) at 425°C. Each mold casting provided two tensile test bars. Thirty-six to forty test bars were obtained for each composition. The test bars were divided into seven sets: one set was directly aged at 155 ± 2°C for 5 h followed by air cooling (i.e., T5 treatment), the other six sets were solution heat-treated at 500 ± 2°C for times up to 24 h (at intervals of 4 h), then quenched into warm water at 65°C, followed by artificial aging at 155 ± 2°C for 5 h (i.e., T6-tempered). The heat-treated test bars were pulled to fracture at room temperature at a strain rate of 4×10^{-4}/s using an Instron Universal testing machine. A strain gauge extensometer was attached to the test bar to measure percentage elongation as the load was applied. The yield strength (YS) was calculated according to the standard 0.2% offset strain, and the elongation was calculated as the percent elongation (%El) over a 50 mm

TABLE I Chemical compositions of the alloys used in the present work

	Chemical composition (wt%)												
Alloy code	Si	Fe	Cu	Mn	Mg	Cr	Ni	Zn	B	Be	Sr	Ag	Ti
M0[a]	11.90	.88	.875	.210	.082	.017	.017	.340	.008	.000	.002	.000	.052
M1[b]	11.74	.793	.875	.211	.086	.026	.020	.338	.008	.000	**.030**	.000	.051
M2	11.79	.789	.867	.206	**.411**	.018	.019	.343	.007	.000	**.026**	.000	.050
M2N	11.46	.749	.878	.199	**.422**	.017	.023	.334	.007	.000	.000	.000	.050
M2B	11.72	.761	.867	.196	**.446**	.018	.024	.324	.007	**.018**	**.025**	.000	.051
M3	11.74	.800	**2.64**	.193	.070	.040	.022	.321	.008	.000	**.039**	.000	.051
M3N	11.76	.798	**2.66**	.195	.067	.040	.022	.331	.008	.000	.000	.000	.051
M4[c]	11.28	.751	**2.61**	.184	**.379**	.033	.027	.313	.007	.000	**.041**	.000	.052
M4N	11.28	.751	**2.61**	.184	**.379**	.033	.027	.313	.007	.000	.000	.000	.052
A	11.65	.722	**2.70**	.182	**.366**	.016	.030	.031	.009	.000	**.025**	**.715**	.050
AB	11.48	.720	**2.73**	.182	**.396**	.017	.032	.309	.009	**.016**	**.034**	**.710**	.050
1NN	11.86	.678	**2.46**	.200	**.314**	.018	**.627**	.241	.002	.000	.000	.000	.050
1N	11.86	.678	**2.46**	.200	**.314**	.018	**.627**	.241	.002	.000	**.021**	.000	.050
2N	11.88	.673	**2.43**	.192	**.378**	.020	**1.41**	.240	.002	.000	**.026**	.000	.050
Z	11.95	.706	**2.81**	.198	**.378**	.019	.029	**2.74**	.002	.000	**.020**	.000	.046
ZN	11.89	.677	**2.66**	.192	**.444**	.019	**.634**	**2.25**	.002	.000	**.021**	.000	.053

[a]Base A413.1 alloy.
[b,c]Reference alloys.

gauge length. The ultimate tensile strength (UTS) was also measured.

One half of each tensile-tested bar was machined to obtain flat surfaces parallel to the loading axis. Hardness measurements were carried out on these surfaces using a Brinell hardness tester with a steel ball diameter of 10 mm (under 50 kgf for 30 s). The average of six readings was taken as the hardness value in each case. The longitudinal sections beneath the fracture surfaces of some of the tensile-tested specimens (M1, M2N, M4, and 2N alloys) were also examined using optical microscopy.

3. Hardness

3.1. Effect of Sr addition

To study the effect of Sr-addition and solution time at 500°C on alloy hardness, the unmodified M0, M2N, M3N and M4N alloys were compared with the Sr-modified M1, M2, M3 and M4 alloys, as shown in Fig. 1 (broken lines vs. solid lines). Strontium additions were made in the range of 260–400 ppm. The results show that in the T5 condition, the decrease in the alloy hardness with Sr addition is less than 13%, due mainly to the change in the morphology of the eutectic Si particles (from brittle, acicular platelets to a rounded fibrous form). Also, Sr leads to a depression in the eutectic temperature causing a shift of the eutectic point to a higher Si content, resulting in an increase in the amount of soft, α-Al formed [1].

After T6 treatment, the hardness values of the Sr-containing M1 (base alloy + 300 ppm Sr) and M3 (2.64% Cu + 390 ppm Sr) alloys overlap with those obtained from the unmodified M0 and M3N alloys. This observation may indicate that neither prolonged solution time nor Sr modification has a marked effect on the precipitation mechanism of Cu phases during ageing at 155°C, after quenching from 500°C. In other words, the Cu phases could have easily dissolved in the matrix after only 4 h of solution treatment at 500°C and reprecipitated thereafter during the ageing process, without being affected by the presence of Sr [15].

However, in the case of the M2 and M4 alloys (containing 0.411% Mg + 260 ppm Sr and 0.379% Mg + 2.61% Cu + 410 ppm Sr, respectively), the effect of Sr addition is significant in lowering the alloy hardness for all solution treatment times. The drop in hardness value of M2 alloy after 8 h solution time is ~6.5% and increases to ~14% after 24 h solution treatment. This can be explained in terms of the coarsening of the Si particles and a consequent decrease in their density (particles/mm^2). In the case of the M4 alloy, the decrease in hardness compared to M4N alloy was approximately constant (~11%), regardless of the solution time. This leads to the conclusion that the hardening effect, caused by precipitation of Mg-containing phases (mainly Mg_2Si and Al_2CuMg) during ageing, was compromised by the softening effect due to the coarsening of the Si particles as well as the increase in the amount of the soft aluminum matrix [1].

Another point of view is that the dissolution of $Al_5Cu_2Mg_8Si_6$ phase during solution treatment is fairly slow (regardless of the Sr concentration). This, in turn, decreases the amounts of free Mg and Cu available for further hardening during the ageing process, as discussed previously [10]. As Fig. 1 shows, the optimum solution time lies close to 8 h for all investigated alloys.

The observations in the present study, of the Sr-modified M2 and M4 alloys exhibiting lower hardness levels compared to the unmodified M2N and M4N alloys, are in contrast to those reported by Shivkumar *et al.* [16] on A356.2 alloys, who found that Sr had no effect on the hardness for alloys solutionized at 540°C for about 27 h. This could be accounted for by the relatively higher solutionizing temperature used in their work compared to that used in the present study (500°C), which would accelerate the decomposition of the as-cast Mg_2Si and its dissolution during solution treatment [17].

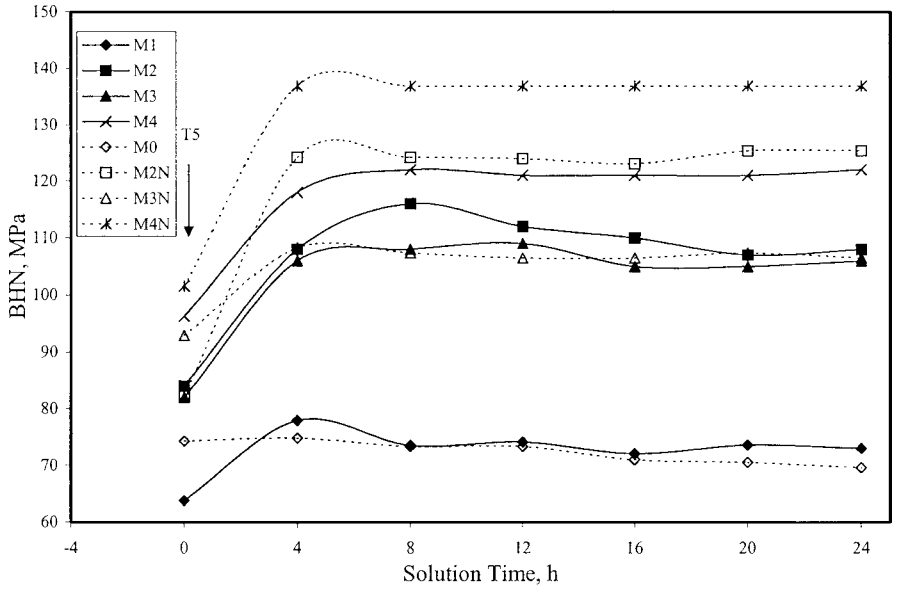

Figure 1 Effect of Mg and Cu additions on the hardness of unmodified and Sr-modified A413.1 alloys treated at different solution times.

TABLE II Hardness and tensile properties of M1 and M4 reference alloys (T6 condition)

Alloy code	Solution time (h)	HBN (MPa)	YS (MPa)	UTS (MPa)	El (%)	Q (MPa)
M1	0 (T5)	63.8	130.2	228.9	3.00	300.5
	4	77.9	135.8	238.7	4.20	332.2
	8	73.5	124.6	234.5	5.90	350.1
	12	74.1	131.6	238.7	5.50	349.8
	16	72.0	124.6	238.0	5.30	346.6
	20	73.6	128.1	242.2	5.20	349.6
	24	73.0	128.8	238.7	5.30	347.3
M4	0(T5)	96.3	175.0	235.9	1.30	253.0
	4	118.0	290.5	330.4	1.24	344.4
	8	122.0	290.0	336.4	1.23	349.9
	12	121.0	290.0	345.0	1.31	362.6
	16	121.0	293.0	352.0	1.35	371.6
	20	121.0	295.0	352.0	1.37	372.5
	24	122.0	295.0	352.0	1.35	371.6

T5 = as-cast followed by ageing at 155°C for 5 h.

TABLE III Differential changes in the mechanical properties of M2, M3 and M4 alloys compared to M1 alloy (T6 condition)

Alloy code	Solution time (h)	ΔHBN (MPa)	ΔYS (MPa)	ΔUTS (MPa)	ΔEl (%)	ΔQ (MPa)
M2	0 (T5)	20.2	25.2	12.6	−0.90	−10.6
	4	30.1	163.8	105.7	−2.90	29.3
	8	42.5	169.4	111.3	−4.30	26.3
	12	37.9	158.9	102.9	−4.00	18.3
	16	38.0	165.9	112.0	−3.60	37.9
	20	33.4	161.0	102.9	−3.50	30.1
	24	35.0	158.2	105.7	−3.80	23.5
M3	0 (T5)	18.2	13.3	2.1	−0.40	−7.2
	4	28.1	102.9	56.0	−2.70	−11.1
	8	34.5	102.2	65.1	−3.70	0.8
	12	34.9	93.8	67.2	−3.40	4.5
	16	33.0	104.3	72.8	−3.10	15.5
	20	31.4	95.2	55.3	−3.00	−0.7
	24	33.0	96.6	74.9	−3.30	11.4
M4	0 (T5)	32.5	44.8	7.0	−1.70	−47.5
	4	40.1	154.7	91.7	−2.96	12.2
	8	48.5	165.4	101.9	−4.67	−0.3
	12	46.9	158.3	106.3	−4.19	12.8
	16	49.0	168.4	114.0	−3.95	24.9
	20	47.4	167.0	109.8	−3.83	22.9
	24	49.0	166.2	113.3	−3.95	24.2

$\Delta HBN = HBN_{M1} - HBN_{alloy}$ (alloy: M2, M3, M4).

3.2. Effect of Mg and Cu addition

The effects of adding of Mg and Cu—individually or combined—on the hardness of both unmodified and Sr-modified 413.1 alloys were also investigated. The Brinell hardness values for the corresponding M2, M3 and M4 alloys as a function of solution treatment time at 500°C are shown in Fig. 1 (solid lines). It is found that increasing the Cu-content in M1 alloy from 0.88% to 2.64% Cu (i.e., M3 alloy) increases the alloy hardness by about 29% in the T5 condition and by 45% in the T6 condition for all solution times up to 24 h, due to the precipitation of $CuAl_2$ from the supersaturated Al matrix.

Magnesium addition (0.41%) to M1 alloy (viz., M2 alloy) exhibited a tendency similar to that of Cu, but gave slightly higher hardness values (the scattering in the results was about ± 4%) than those obtained for the M3 alloy, indicating that the hardening due to Mg_2Si precipitation is more effective than that due to $CuAl_2$. This is also evident from a comparison of the amounts of Cu and Mg present in the two alloys: ∼0.9% Cu and ∼0.4% Mg in M2 alloy vs. ∼2.6% Cu and ∼0.1% Mg in M3 alloy. Compared to M1 alloy, the hardness of M2 alloy increased by ∼32% after T5 treatment, and by ∼50% after T6 treatment.

In M4 alloy (containing ∼2.6% Cu and ∼0.45 Mg), the hardness value is seen to increase markedly—by 51% after T5 treatment, and by 65% after T6 treatment, compared to M1 alloy, as shown in Tables II and III. However, as reported in a previous study [18], the presence of both high Cu and high Mg levels in the alloy is associated with a lower hardness value than would be expected from the sum of their individual additions (i.e., M3 + M2). This may be interpreted in terms of the formation of complex insoluble phases such as $Al_5Mg_8Si_6Cu_2$ [1].

3.3. Effect of Be addition

When Be was added to M2 alloy in small amounts (∼0.02% Be) to prevent Mg oxidation (i.e., MgO and $MgAl_2O_4$ (spinel) formation) during melting, the hardness increased slightly, as shown in Fig. 2. Maximum hardness was attained after 8 h solution treatment, and the improvement in hardness varied between 2.1% and 8.4%, over the range of solution treatment times studied. In another study [19], it was found that addition of Be reduced the alloy sensitivity for hot cracking. Thus, while Be addition may be useful in these respects, however, it does not contribute to the alloy hardness. The other alloy to which Be was added is AB alloy. As Ag, Ni and Zn additions were also made (classifying it under the M4 reference alloy group), the effect of Be for this alloy will be discussed in the next section.

3.4. Effect of Ag, Ni, and Zn addition

Addition of 0.7% Ag to M4 alloy (i.e., A alloy) had no significant effect on the alloy hardness. However, when Be was added together with Ag, ΔHBN became more positive and peak hardness was achieved after only 4 h solution treatment (ΔHBN = 8.8 MPa), as shown in Table IV. Addition of nickel up to 1.41% (2N alloy) to M4 alloy improved the alloy hardness in the T5 condition. However, this was not the case after T6 treatment, where the hardness decreased markedly compared to that obtained from M4 alloy under similar heat treatment conditions, as shown in Table V. On the other hand, with Zn and Zn + Ni additions (i.e., Z and ZN alloys, respectively), a better hardness was obtained in both T5 and T6 conditions, for solution treatment times less than 20 h, Table V (a difference of ∼2 MPa is considered as data scatter).

Hardening with addition of Zn is more pronounced in alloys containing high Mg levels, due to the precipitation of $Mg_3Zn_3Al_2$ phase, provided the Mg content

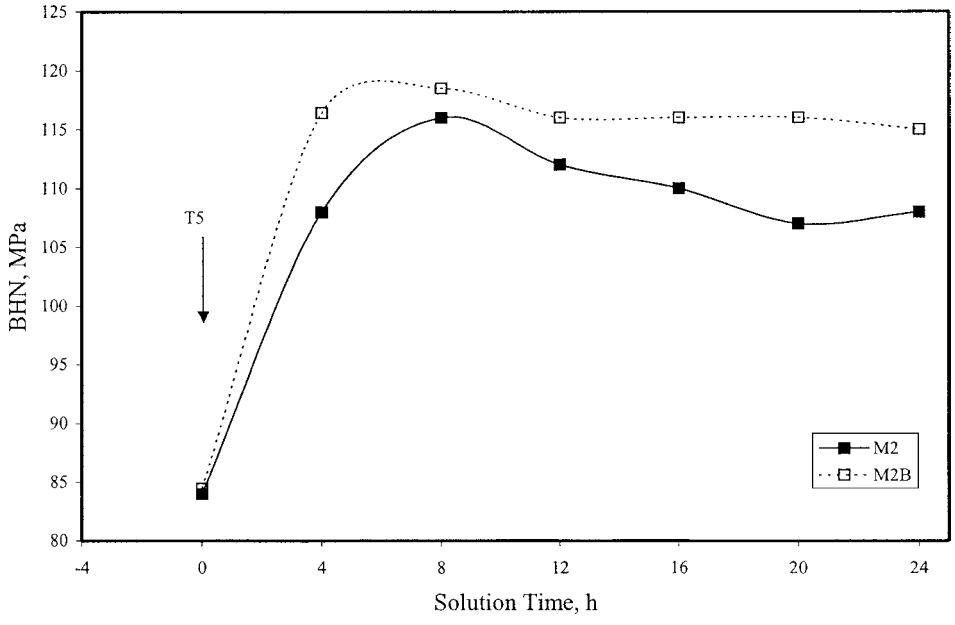

Figure 2 Effect of Be addition on the hardness of M2 alloy as a function of solution time.

is sufficiently high, as in the case of 7XXX alloys [20], which contain Mg in the order of 2%. In the M4 alloy, while a Mg content of ~0.4% may not be high enough to show a significant increase in hardness, some improvement is nevertheless observed with the addition of Zn (in the Z alloy). Another possibility can be the precipitation of Cu_3ZnAl_3 [20]. It has been reported [21] that Zn up to 3% has no pronounced effect on the properties of Al-Si alloys. The role of Zn in cast Al-Si alloys is not well understood, except for its effect in improving the alloy machinability [22].

Addition of up to 2.5% Ni is known to increase the ability of an alloy to resist the effects of exposure to elevated temperatures. For example, additions of 1 to 2% Ni to 2xxx and 3xxx alloys imparts high tensile properties to these alloys at elevated temperatures [20]. Thus, the combined precipitation of $Mg_3Zn_3Al_2$, Cu_3ZnAl_3, and Cu_3NiAl_6 may explain the better hardness observed in the ZN alloy compared to the M4 reference alloy.

TABLE IV Differential changes in the mechanical properties of A and AB alloys compared to M4 alloy (T6 condition)

Alloy code	Solution time (h)	ΔHBN (MPa)	ΔYS (MPa)	ΔUTS (MPa)	ΔEl (%)	ΔQ (MPa)
A	0 (T5)	−0.3	16.1	29.4	0.2	38.7
	4	1.5	46.9	37.1	−0.09	32.2
	8	2.0	14.5	−1.7	−0.23	−15.2
	12	1.0	16.0	−7.6	−0.31	−25.2
	16	0.0	24.1	−3.4	−0.25	−16.7
	20	1.0	4.5	−17.4	−0.37	−37.9
	24	0.0	1.8	−27.2	−0.35	−46.8
AB	0 (T5)	2.7	7.7	5.6	0.05	8.1
	4	8.8	19.6	11.2	−0.11	5.1
	8	3	18.0	14.4	−0.08	10.0
	12	2.5	20.2	0.1	−0.11	−5.6
	16	2	31.1	14.8	−0.07	11.4
	20	2	16.5	−9.0	−0.27	−23.3
	24	1.6	8.1	−9.0	−0.25	−22.4

4. Tensile properties

4.1. Effect of Sr addition

Fig. 3 shows the variation in tensile properties, (i.e., YS, UTS, and % El) and quality index (Q) of the unmodified M2N alloy (containing 0.422% Mg) and the modified M2 alloy (containing 0.411% Mg + 260 pm Sr) as a function of solution time. The concept of the quality index (Q) was developed by Drouzy *et al.* [23]

TABLE V Differential changes in the mechanical properties of 1N, 2N, ZN and Z alloys compared to M4 alloy (T6 condition)

Alloy code	Solution time (h)	ΔHBN (MPa)	ΔYS (MPa)	ΔUTS (MPa)	ΔEl (%)	ΔQ (MPa)
1N	0 (T5)	2.2	4.9	−6.3	−0.1	−11.5
	4	1	−31.5	−28.0	−0.14	−35.8
	8	−3.5	−28.2	−43.7	−0.16	−52.8
	12	−5	−25.3	−44.0	−0.23	−56.5
	16	−5	−31.2	−46.1	−0.25	−59.4
	20	−6	−33.3	−45.4	−0.17	−54.0
	24	−8	−33.2	−41.2	−0.1	−46.2
2N	0 (T5)	3.7	15.4	−2.1	−0.2	−13.0
	4	−6	−28.7	−23.1	−0.25	−37.8
	8	−5	−24.7	−37.5	−0.29	−55.0
	12	−3	−23.9	−37.0	−0.31	−54.6
	16	−3	−27.0	−42.6	−0.29	−58.3
	20	−4	−28.0	−39.8	−0.22	−51.2
	24	−4	−27.6	−38.4	−0.22	−50.0
ZN	0 (T5)	0	29.4	−14.0	−0.3	−31.1
	4	1	6.3	−25.9	−0.38	−49.7
	8	6.8	20.1	−9.4	−0.38	−33.5
	12	5.4	18.1	−22.3	−0.41	−46.7
	16	1	−6.0	−40.5	−0.35	−60.0
	20	0	−21.4	−38.4	−0.17	−47.0
	24	−2	−23.4	−37.7	−0.15	−45.4
Z	0 (T5)	3	13.3	10.5	0.1	15.3
	4	1	6.3	7.0	−0.04	4.9
	8	3	24.3	11.6	−0.08	7.2
	12	4	21.6	−6.9	−0.21	−18.2
	16	0	−2.5	−33.5	−0.25	−46.8
	20	−1	−17.2	−35.6	−0.27	−49.9
	24	−3	−16.4	−36.0	−0.25	−49.3

as a means of simplifying the influence of the many variables involved during casting on the tensile properties. From a consideration of the relationship between the tensile parameters of Al-Si-Mg alloys, they defined the quality index (Q) as:

$$Q\,(\text{MPa}) = \text{UTS}\,(\text{MPa}) + 150 \log\,(\%\text{El})$$

where the coefficient 150 corresponds to that obtained for heat-treated 356 (Al-6%Si-0.35%Mg) alloys.

In the present study, the M2N alloy displayed higher YS and UTS values than the M2 alloy (Fig. 3a and b), in general, and lower percentage elongation (%El) and Q values (Fig. 3c and d). As expected, the yield strength of M2N alloy in the T5 condition is higher than that of M2 alloy due to the changes in the Si particle characteristics caused by Sr modification.

The difference in YS values after solution treatment decreased to a minimum in the 4–8 h solution time range. This can be explained in terms of the mechanism of transformation of the Si particle morphology from acicular or fibrous form (depending on the solidification rate) to globular form through the fragmentation, spheroidization and coarsening processes occurring during solution treatment, as discussed previously. Therefore, it is expected that the spheroidization process in M2N alloy is still not completed after 8 h (due to the relatively low solutionizing temperature), while in the M2 (modified) alloy the fragmentation and spheroidization stages are completed, with the commencement of the coarsening stage.

After 16 h solution treatment, the gap between YS curves for M2N and M2 alloys increased, when the second stage (Si coarsening) in M2N alloy started, as shown in Fig. 3a. Li et *al.* [24] reported that the spheroidization of modified A356.0 alloys is essentially complete after 1 h of solution treatment at 540°C, while in unmodified alloys, complete spheroidization is not achieved even after 12 h. The data of Parker *et al.* [25] also indicates that in the modified samples, a high degree of spheroidization occurs only after 10 min at 540°C.

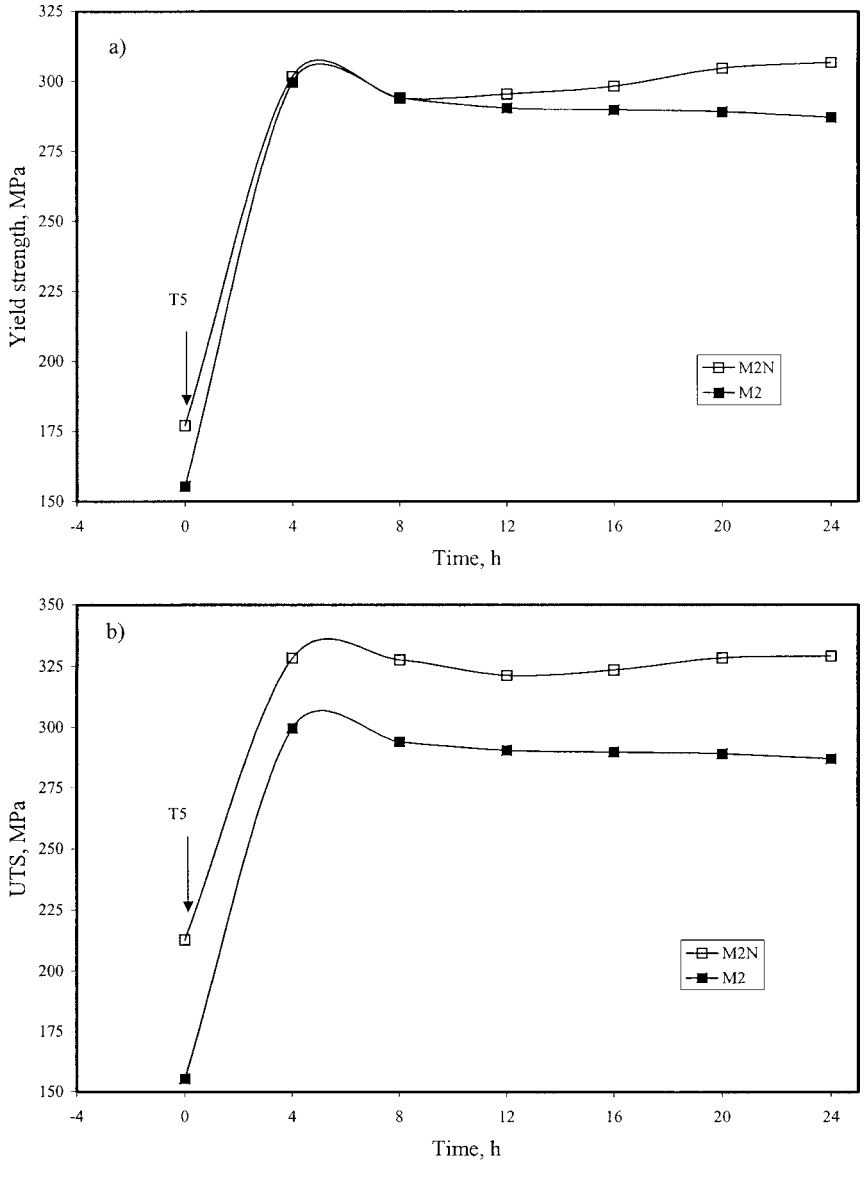

Figure 3 Dependence of the mechanical properties of M2N and M2 alloys on solution time at 500°C: (a) YS, (b) UTS, (c) %El, and (d) Q-factor. (*Continued*)

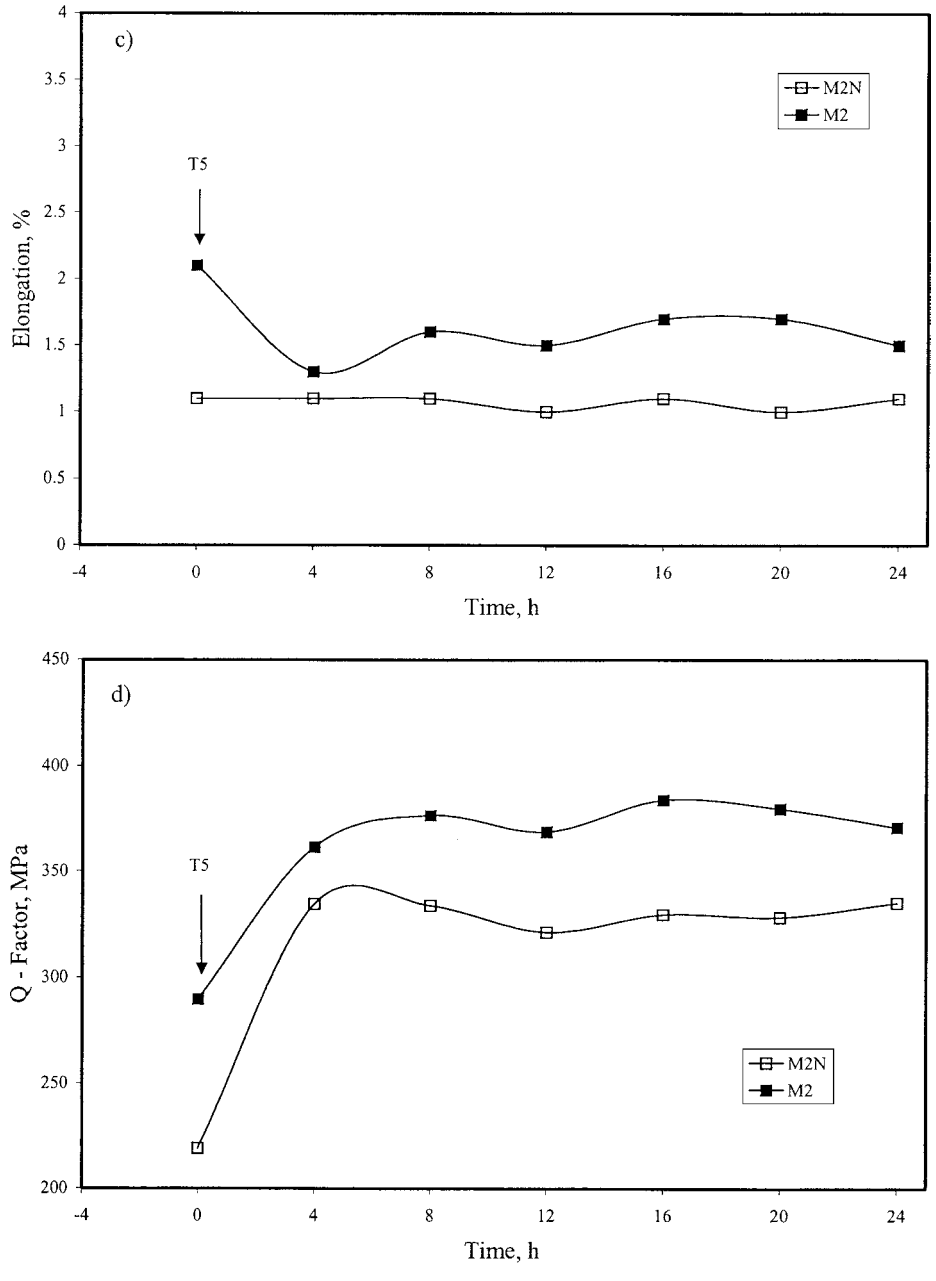

Figure 3 (*Continued*).

The difference in UTS and %El between M2N and M2 alloys is much more obvious than that observed for YS. In other words, the yield strength is less sensitive to the changes in the microstructure or the presence of Sr. Saigal and Berry [26] have shown that the stress required for localized yielding varies marginally with the Si particle size or the aspect ratio. For example, increasing the aspect ratio or particle size by a factor of four reduces the yield stress by about 5%.

The quality index, which summarises the tensile properties, shows that the modified M2 alloy exhibits higher Q values than the unmodified M2N alloy for all solution treatment times, as shown in Fig. 3d. The improvement in Q values upon modification and solution treatment can be attributed to the increase in %El. The high values of ductility in modified alloys make it possible to maintain Q at a constant value and alter the aging cycle to increase the UTS [24].

4.2. Effect of Mg and Cu addition

The tensile data for the M1 and M4 reference alloys at various solution treatment times are listed in Table II, while the differential changes in the mechanical properties of M2, M3, and M4 alloys with respect to M1 alloy are listed in Table III. As all the tensile property curves obtained resembled those shown in Fig. 3, the effect of various element additions on the properties of the reference alloys are discussed directly with respect to Tables II to V in this and the following section.

From Tables II and III, it can be seen that the YS and UTS of M1 alloy are approximately constant regardless of the solution treatment time and possess the lowest values. The average values of YS and UTS are 129 MPa $\pm$ 4% and 237 MPa $\pm$ 3%, respectively. The percentage elongation of M1 alloy, however, increases from 3% in the T5 condition to $\sim$5.5% after 8 h solution time at 500°C (T6 condition), and levels off thereafter (Table II). The increase in %El of $\sim$83% can be

interpreted in terms of the removal of the internal stresses stored in the alloy during casting. Such an increase would, in turn, noticeably affect the Q value, as shown in Table II.

When 2.64% Cu was added to the M1 alloy (i.e., M3 alloy), the tensile properties improved significantly, especially when the solution treatment time exceeded 4 h, as can be seen from Table III. The YS of M3 alloy in the T5 condition was ~10% higher than that of the M1 alloy (Table II) and increased further by ~75% in the T6 condition (for solution times of 4 h or more). The same trend was observed for UTS, with an increase of ~30% being observed. The percentage elongation, however, decreased by about 13% in the T5 condition, and by ~60% when the solution time exceeded 8 h (prior to quenching and aging at 155°C for 5 h), as shown in Table III.

The modified M2 alloy (with 0.41% Mg) revealed the same tendency as that shown by the M3 alloy (compared to M1 alloy) but exhibited higher values. For example, after T5 treatment, the YS and UTS of M2 alloy increased by ~19% and ~6%, respectively, while %El decreased by ~27%. After 4 h solution time (prior to quenching and aging), the YS and UTS of M2 alloy were increased by ~125% and ~45%, respectively, whereas %El decreased by ~70%. As discussed in Section 3.2, these results also support the conclusion that addition of 0.41% Mg improves the tensile strength more than the addition of 2.64% Cu. The quality index values shown in Table III also reveal that M2 alloy has the highest values compared to other alloys in this group (reference alloy M1) in the T6 condition.

Simultaneous additions of 0.38% Mg and 2.61% Cu to the M1 alloy (i.e., M4 alloy) produced approximately the same levels of tensile properties as those obtained from M2 alloy, as depicted in Table III. This observation can be attributed to the interaction between Cu and Mg to form $Al_5Cu_2Mg_8Si_6$ phase. As mentioned previously, this phase does not undergo complete dissolution upon solution treatment, even after 24 h. Also, due to its formation, not all of the Cu and Mg that were added to the alloy are available during the artificial aging process.

However, although the properties of M4 (Mg + Cu-containing) alloy are still higher than those of M3 (Cu-containing) alloy, the presence of both Mg and Cu is important as it improves the dimensional stability (after heat treatment) and bearing characteristics of the alloy, in addition to the high strength and hardness at elevated temperatures [20].

4.3. Effect of Ag, Ni, and Zn addition

To study the effect of addition of Ag, Be, Ni, and Zn on the alloy performance, the Sr-modified M4 alloy was taken as the reference alloy. The elements were added individually or in combination in the required amounts to the M4 alloy, to give the compositions listed in Table I. The differential changes in the mechanical properties and Q values of A and AB alloys (containing Ag and Ag + Be, respectively) with increase in solution time are given in Table IV. The data shows that addition of Ag and Be increases the YS of these alloys. The maximum increase (~16%) for A alloy was achieved after 4 h solution time while that for AB alloy (10%) was obtained after 16 h. However, as can be seen from Table IV, the addition of Ag + Be resulted in more stable YS values with respect to solution times beyond 4 h, providing a means to reduce the heat treatment cycle [27]. In general, addition of Ag is known to substantially increase the strength of heat-treated (fixed solutionizing time) and aged Al-Cu-Mg alloys [20].

The UTS value of A alloy increased by ~12% after T6 treatment (with 4 h solution time). Thereafter, a continuous decrease in the UTS occurred with increasing solution time. In the case of the AB alloy, the UTS value remained higher than the corresponding M4 alloy UTS up to 16 h solution time, then decreased with further solution time to give values lower than the UTS obtained from M4 alloy. These observations can be attributed to the coarsening of the Si particles after prolonged solution treatment, particularly in Sr-modified alloys. Percentage elongation values of A and AB alloys were less than those corresponding to the M4 alloy for all solution times. Addition of Be, however, improved the influence of Ag addition on the percentage elongation, as observed from the high Δ%El values of AB alloy compared to A alloy, Table IV.

Thus, while the addition of Ag is very effective after T5 treatment, and optimizes the alloy strength after 4 h solution treatment (T6 treatment), a combined Ag + Be addition (i.e., AB alloy) improves the mechanical properties of the M4 alloy in the T6 condition more than the addition of Ag alone, at solution times longer than 4 h. This observation can be attributed to the fact that Be reduces the amount of Mg losses during the melting process. This would enhance the increase in the amount of strengthening precipitates (i.e., Mg_2Si) coupled with a decrease in the size of the Si particles through the fragmentation process.

In their study on the effect of Be on the properties of A357.0 castings, Granger *et al.* [28] have reported that the presence of Be reduces oxidation of Mg at elevated temperature and prevents the formation of $Al_{10}Mg_4Si_4Be$ phase which diminishes the amount of Mg available to form Mg_2Si (i.e., the strengthening phase).

Also, during solidification, the presence of Be assists in modifying the morphology of the iron intermetallics from the deleterious plate-like β-Al_5FeSi phase to the comparatively less harmful compact Chinese-script α-Al_8Fe_2Si phase (with respect to the alloy properties), as reported in the literature [29, 30]. Similar observations have been documented by Samuel *et al.* [31] and Murali *et al.* [32, 33] in the case of A319.2 and 356 alloys, respectively.

Table V displays the effect of Ni and Zn additions on the mechanical properties of M4 alloy at different solution treatment times. Nickel addition (i.e., 1N, 2N alloys) resulted in increasing the alloy YS and UTS values after T5 treatment according to the amount of Ni added, and a corresponding decrease in both %El and Q values. In the T6 condition, with increase in solution time up to 24 h, the YS, UTS, %El, and Q levels for 1N

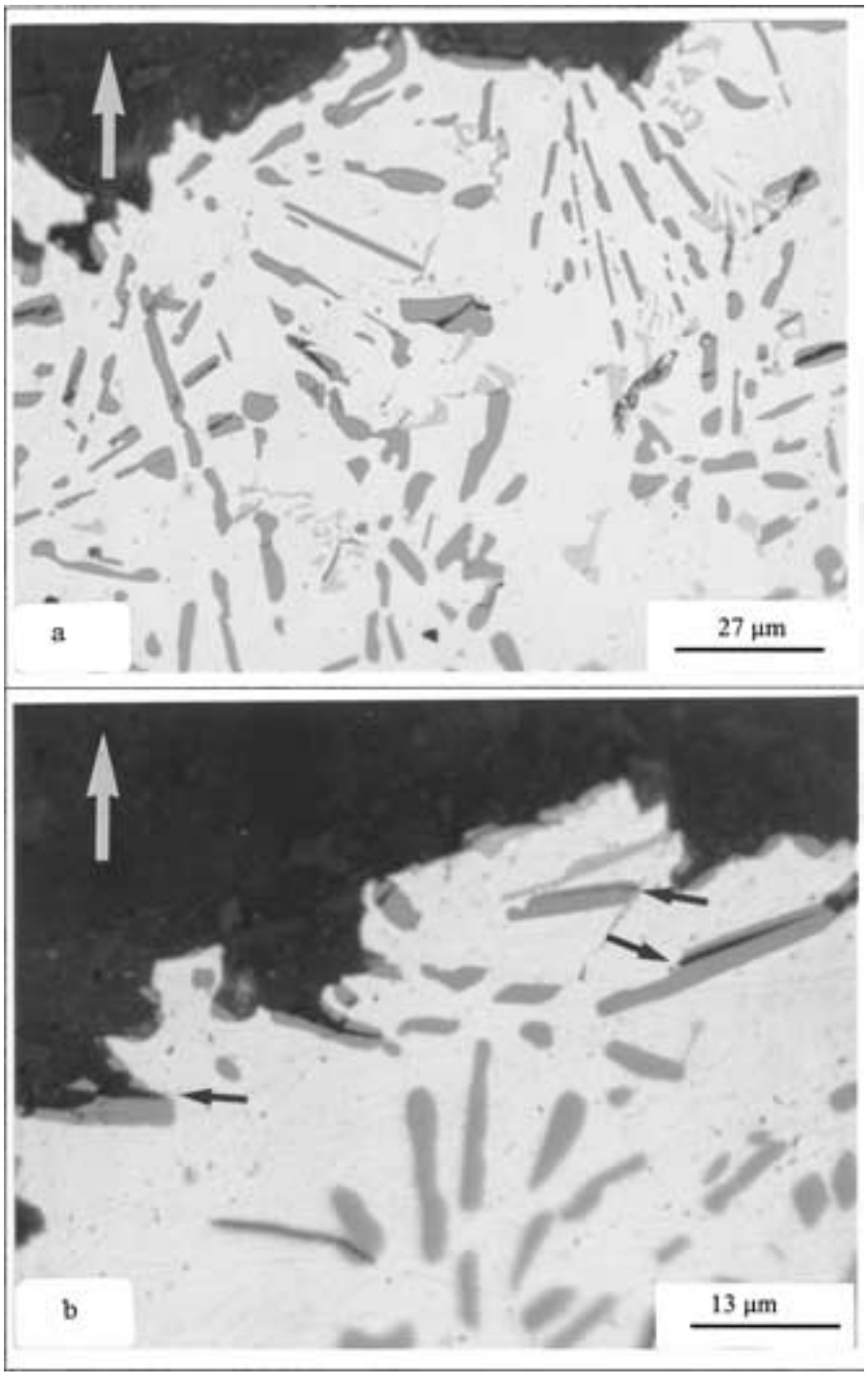

Figure 4 Microstructure beneath the fracture surface in unmodified M2N alloy, solution heat-treated at 500°C for 8 h. White arrows in Figs 4 through 6 indicate the loading direction.

and 2N alloys were much lower than the corresponding values obtained for the M4 alloy treated similarly. These results can be attributed to the formation of stable complex intermetallics due to the combination of Ni with Cu, which appear in the form of Chinese script particles. This process is expected to reduce the amount of Cu available to form Al_2Cu, which represents the main strengthening phase during the aging treatment [34].

Addition of 2.74% Zn to M4 alloy (i.e., Z alloy) increased the alloy YS levels in the T6 condition (following solution times up to 12 h) to above those obtained from the M4 reference alloy under similar heat treatment conditions. Further increase in solution time resulted in reducing the yield strength successively. The UTS of Z alloy was relatively higher than that of M4 alloy up to only 8 h, while %El of Z alloy was less than that of M4 alloy for solution times of 12 h and above. It should be mentioned here that in the T5 condition, the Z alloy possessed a yield strength and quality index much superior to that of M4 alloy, whereas in the T6 condition, optimum strength and Q-values were obtained after 8 h solution treatment time (cf. M4 alloy for the same conditions).

When Zn and Ni were added together to M4 alloy (i.e., ZN alloy), the mechanical properties obtained were lower than those of Z alloy for all solution treatment times. Thus, it may be concluded that addition of Zn alone improves the mechanical properties of M4

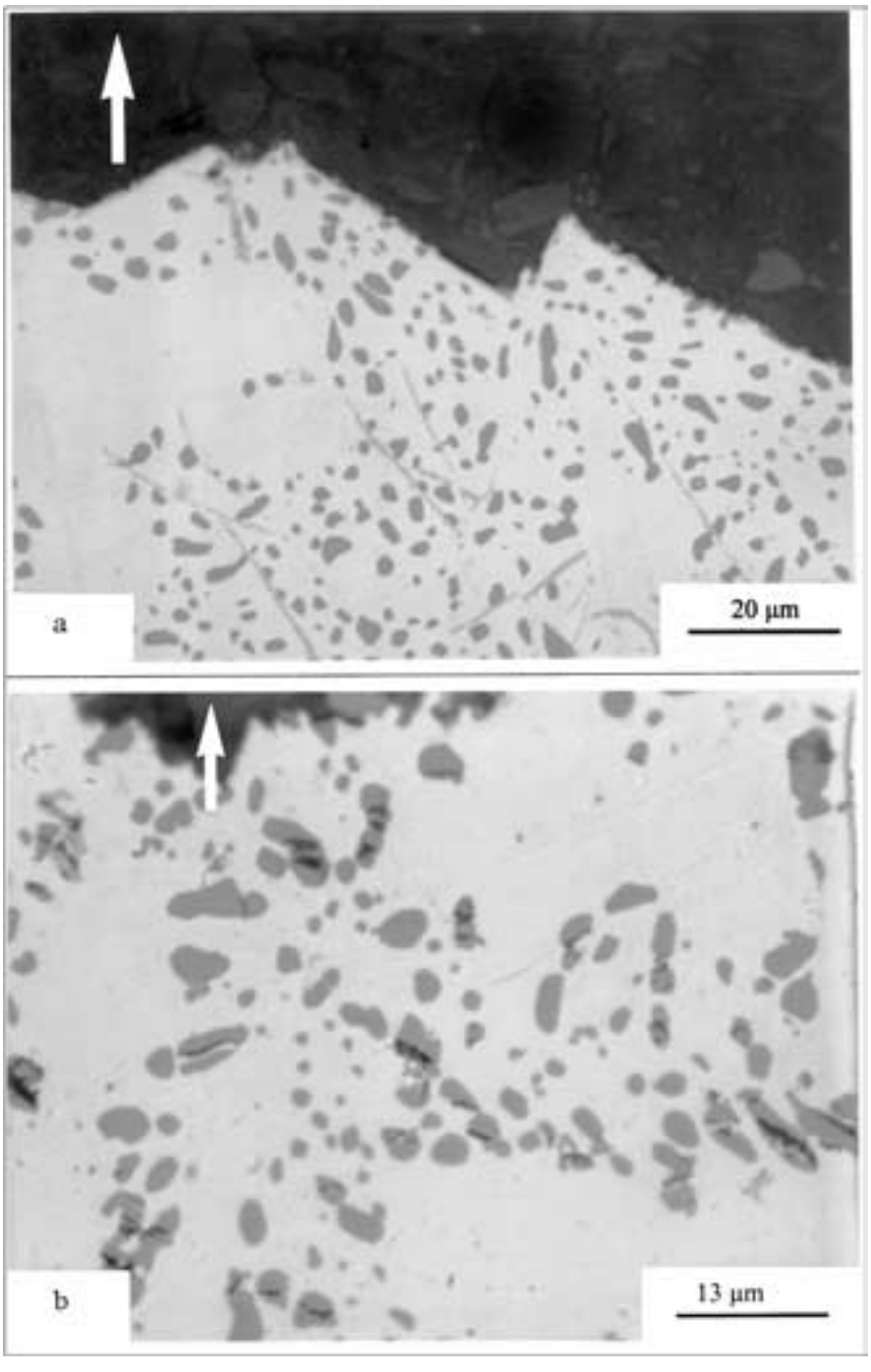

Figure 5 Microstructure beneath the fracture surface in Sr-modified: (a) M1 and (b) M4 alloys, solution heat-treated at 500°C for 8 h.

alloy, and reduces the required solution time to 8 h (or less). It is important to note that after 24 h at 500°C, all the mechanical properties of 1N, 2N, ZN and Z alloys exhibited more or less the same levels (as shown in Table V).

4.4. Microstructure beneath the fracture surface

Longitudinal sections normal to the fracture surface of the tensile-tested alloy samples were examined to determine the mode of crack propagation beneath the fracture surface. The fractured test bars were cut into two halves (transverse to the fracture plane). The sections were mounted and polished for microstructural examination using optical microscopy. Fig. 4 shows the microstructures near the fracture surface of the sample sectioned from M2N alloy (in the unmodified condition), solution heat-treated at 500°C for 8 h before pulling to fracture. It can be seen from the microstructure that cracks occur within the brittle acicular Si particles, Fig. 4a. These cracks are more or less perpendicular to the loading axis (thick white arrow). The arrows in Fig. 4b indicate that the cracks were prevented from propagating into the surrounding aluminum matrix due to its high plasticity. It is also worth noting that the cracks pass through the Si particles themselves, and not at their interfaces with the aluminum matrix. These observations are in agreement with the work of Powell [35], but in contrast to the findings of Lebyodkin *et al.* [36], who explained the fracture effect in terms of the decohesion between the silicon plates and the matrix.

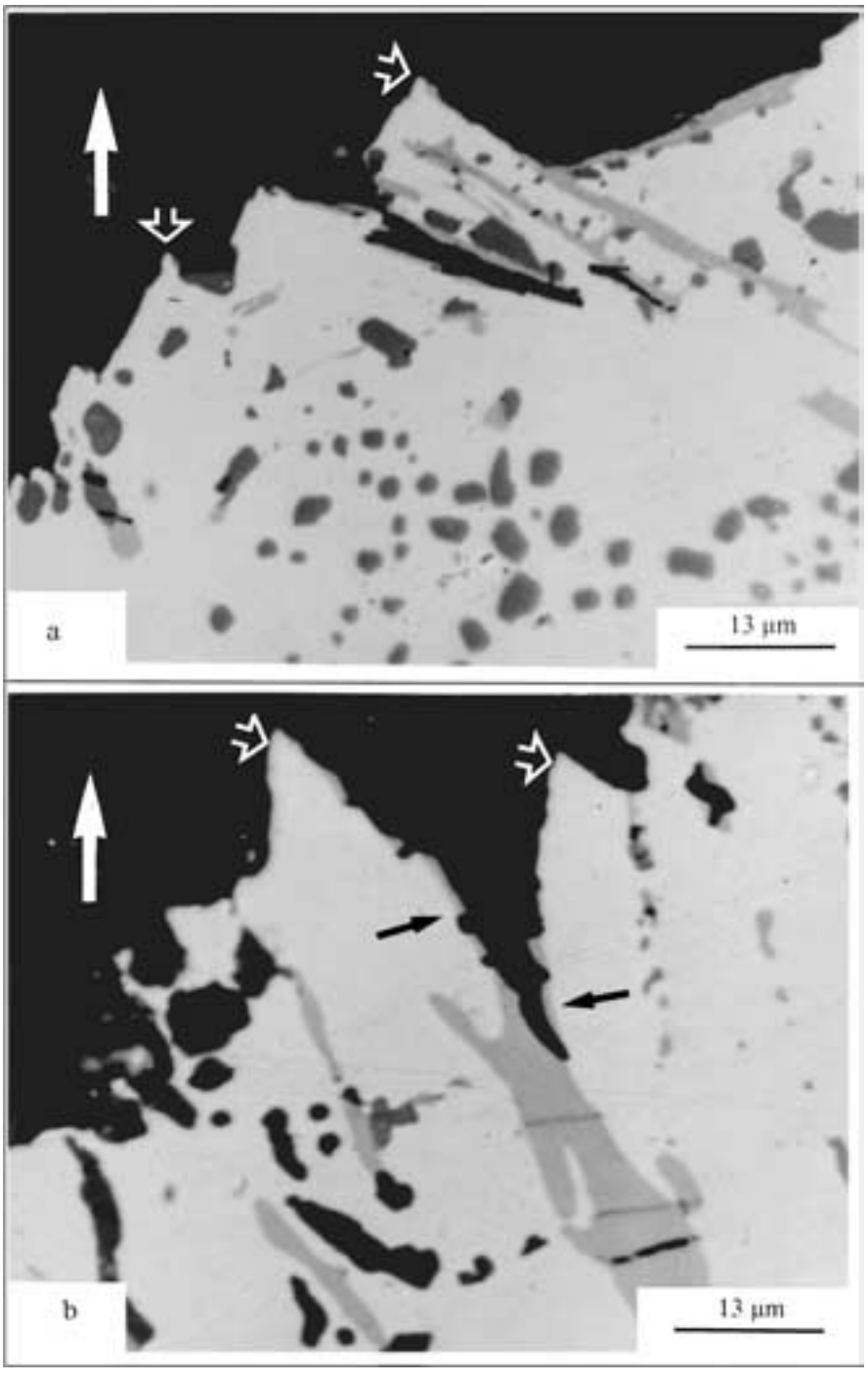

Figure 6 Microstructure beneath the fracture surface in Sr-modified: (a) M4 and (b) 2N alloys, solution heat-treated at 500°C for 8 h. Black arrows indicate the propagation of the secondary crack within the intermetallic phase particle beneath the fracture surface. Open white arrows show the pinpoint form of the α-Al dendrites, revealing their high ductility during plastic deformation.

In the case of the Sr-modified M1 base alloy (following solution treatment at 500°C for 8 h), the Si particles were fragmented, spheroidized, and less interconnected with each other than in the case of unmodified alloys, as shown in Fig. 5a. Therefore, during the rupture process, cracks propagated through the interdendritic regions, as seen from the figure. With the addition of 2.61% Cu and 0.38% Mg to Sr-modified M4 alloy, the corresponding hardness and strength (YS, UTS) were significantly increased (Table III), resulting in the shearing of a larger number of Si particles, extending to regions well below the fracture surface, Fig. 5b. Shivkumar *et al.* [16] have reported that the microhardness of the matrix is increased by more than 20% of its initial value due to substantial straining, before failure occurs.

The primary and secondary cracks can also propagate through the intermetallic phases, as illustrated in Fig. 6, where the longitudinal sections below the fracture surfaces of the Sr-modified M4N and 2N alloys, solution heat-treated at 500°C/8 h, are shown as examples. The pin-point form of the α-Al dendrites (see open arrows in Fig. 6), indicates their ductile nature. It should be noted here that the black spots in Fig. 6 might be due to Si particles pulled out during polishing. These observations confirm the theoretical studies by Gurland and

Gangulee [37] that the fracture in Al-Si alloys occurs in three stages:

(i) Crack initiation at the Si particles;
(ii) Propagation of cracks in the interdendritic regions; and
(iii) Rupture of the Al matrix.

5. Conclusions

1. Addition of Sr decreases the hardness and strength (YS, UTS) of the Mg-containing alloys, which could probably arise from a retardation of the precipitation of Mg_2Si during the aging process (i.e., increasing the incubation period prior to the commencement of precipitation), regardless of the solution time at 500°C. Transmission electron microscopic examination is required to confirm this suggestion. The copper-containing alloys, however, are less sensitive to the presence of Sr.

2. All alloying element additions, i.e., Mg, Cu, Be, Ag, and Zn result in improving the hardness and strength of the base alloy, especially in the T6 condition. Addition of Ni (up to 1.41%), however, decreases the hardness and tensile properties (YS, UTS and %El) of the alloy. This may be interpreted in terms of the formation of intermetallics which may control the grain size, rather than contribute to the hardening of the heat-treated alloys.

3. In unmodified alloys, cracks initiate within the brittle acicular Si particles themselves, without passing through the ductile Al matrix, whereas in modified alloys, the cracks propagate through interdendritic regions, leading to the deformation of the α-Al dendrites, their pinpoint shapes indicating their ductile nature.

4. The number of cracked Si and intermetallic particles beneath the fracture surface increases with the increase in the ultimate tensile strength of the alloy. The latter is a function of the type and amount of alloying elements added.

Acknowledgements

Financial and in-kind support received from the Natural Sciences and Engineering Research Council of Canada (NSERC), General Motors Powertrain (U.S.A.), Corporativo Nemak (Mexico), and the Centre Québécois de Recherche et de Développement de l'Aluminium (CQRDA) is gratefully acknowledged. The authors would like to thank MM Glenn Poirier and Lang Shi of the Microanalysis Laboratory, Earth and Planetary Science, McGill University for carrying out the EPMA analysis, C. McLaughlin, Documentation Consultant (UQAC) for valuable assistance, and Dr. A.M. Samuel for a critical review of the manuscript. Also, Dr. M.A. Moustafa wishes to acknowledge the Central Metallurgical Research and Development Institute (CMRDI), Egypt for leave of absence.

References

1. M. A. MOUSTAFA, F. H. SAMUEL and H. W. DOTY, *J. Mater. Sci.* **38** (2003) 4543.
2. K. KANEKO, S. HAYASHI, A. MOCHIZUKI, M. AONO, K. IKEDA and K. TOYOSE, *JSAE Rev.* **15**(4) (1994) 367.
3. T. A. BARNES and I. R. PASHBY, *Pt I & II, J. Mater. Proc. Techn.* **99**(1–3) (2000) 62, 72.
4. H. NAKANISHI, K. KAKIHARA, A. NAKAYAMA and T. MURAYAMA, *JSAE Rev.* **23**(3) (2002) 365.
5. T. DESAKI and S. KAMIYA, *ibid.* **21**(1) (2000) 143.
6. P. KAPRANOS, D. H. KIRKWOOD, H. V. ATKINSON, J. T. RHEINLANDER, J. J. BENTZEN, P. T. TOFT, C. P. DEBEL, G. LASLAZ, L. MAENNER, S. BLAIS, J. M. RODRIGUEZ-IBABE, L. LASA, P. GIORDANO, G. CHIARMETTA and A. GIESE, *J. Mater. Proc. Techn.* **135**(2/3) (2003) 271.
7. W. S. MILLER, L. ZHUANG, J. BOTTEMA, A. J. WITTEBROOD, P. DE SMET, A. HASZLER and A. VIEREGGE, *Mater. Sci. Engng.* A **280**(1) (2000) 37.
8. T.-S. SHIH and F.-S. SHIH, *Int. J. Cast Met. Res.* **10** (1998) 273.
9. A. M. SAMUEL, P. OUELLET, F. H. SAMUEL and H. W. DOTY, *AFS Trans.* **105** (1997) 951.
10. C. W. MEYERS, K. H. HINTON and J. S. CHOU, *Mater. Sci. Forum* **102–104** (1992) 75.
11. D. APELIAN, S. SHIVKUMAR and G. SIGWORTH, *AFS Trans.* **97** (1989) 727.
12. O. ENGLER and J. HIRSCH, *Mater. Sci. Engng.* A **336**(1/2) (2002) 249.
13. M. JAIN, J. ALLIN and M. J. BULL, *Mater. Sci. Engng.* A **256**(1/2) (1998) 69.
14. H. HAYASHI and T. NAKAGAWA, *J. Mater. Proc. Techn.* **46**(3/4) (1994) 455.
15. Alloy Digest, Data on Worldwide Metals and Alloys, May 1985.
16. S. SHIVKUMAR, S. RICCI, JR., B. STEENHOFF, D. APELIAN and G. SIGWORTH, *AFS Trans.* **97** (1989) 791.
17. J. F. MONDOLFO, "Aluminum Alloys: Structure and Properties" (Butterworth and Co., London, 1976).
18. M. A. MOUSTAFA, F. H. SAMUEL, H. W. DOTY and S. VALTIERRA, *Int. J. Cast Met. Res.* **14** (2002) 235.
19. GHOLAMALI F. C. MORVARI, M. Eng. Thesis, UQAC, Chicoutimi, Canada, October 1999.
20. J. E. HATCH, "Aluminum: Properties and Physical Metallurgy" (American Society for Metals, Metals Park, OH, 1984).
21. R. W. BRUNER, "Die Casting Alloys" (SDCE Supplement, Warren, MI, 1976).
22. D. L. COLWELL, *AFS Trans.* **60** (1952) 87.
23. M. DROUZY, S. JACOB and M. RICHARD, *AFS Int. Cast Met. Res. J.* June (1980) 43.
24. H. J. LI, S. S. SHIVKUMAR, X. J. LUO and D. APELIAN, *Cast Met.* **1** (1989) 227.
25. B. A. PARKER, D. S. SAUNDERS and J. R. GRIFFITHS, *Met. Forum* **5** (1982) 48.
26. A. SAIGAL and J. BERRY, *AFS Trans.* **93** (1983) 699.
27. C. LEPAGE, M. Eng. Thesis, UQAC, Chicoutimi, Canada, 2002, Unpublished results.
28. D. A. GRANGER, R. R. SAWTELL and M. M. KERSKER, *AFS Trans.* **92** (1984) 579.
29. P. S. WANG, Y. J. LIAUH, S. L. LEE and J. C. LIN, *Mater. Chem. Phys.* **53** (1998) 195.
30. S. MURALI, A. TRIVEDI, K. S. SHAMANNA and K. S. S. MURTHY, *Mater. Eng. Perform.* **5** (1996) 462.
31. A. M. SAMUEL, F. H. SAMUEL, C. VILLENEUVE, H. W. DOTY and S. VALTIERRA, *Int. J. Cast Met. Res.* **14** (2001) 97.
32. S. MURALI, K. S. RAMAN and K. S. S. MURTHY, *Mater. Sci. and Engng.* A **190** (1995) 165.
33. *Idem.*, *Cast Met.* **6** (1994) 189.
34. M. A. MOUSTAFA, C. LEPAGE, F. H. SAMUEL and H. W. DOTY, *Int. J. Cast Met. Res.* **15** (2003) 609.
35. G. W. POWELL, *Mater. Character.* (1994) 275.
36. M. LEBYODKIN, A. DESCHAMPS and Y. BRECHET, *Mater. Sci. Engng.* (1997) 481.
37. A. GANGULEE and J. GURLAND, *Trans. Met. Soc. AIME* **239** (1967) 239.

Received 4 February
and accepted 5 August 2003